Green Chemistry

PAPER

Published on 17 June 2026

Cite this: DOI: 10.1039/d6gc02190e

Scalable electrochemical Clemmensen-type deoxygenation of aromatic aldehydes and ketones

Eva Plut, [a] Rok Narobe, [a] Theertha Babu Therambil,[a] Marcel Nicolas Perner, [a] Sebastian Kissel, [a] Tomas Horsten, [a] Nicola C. Aust[b] and Siegfried R. Waldvogel *[a,c]

Received 11th April 2026,
Accepted 16th June 2026

DOI: 10.1039/d6gc02190e

rsc.li/greenchem

Deoxygenation is an important approach for the conversion of abundant, oxygen-rich biomass-based compounds into higher value-added chemicals, typically performed under harsh reaction conditions producing excessive amounts of reagent waste. We report a mild, operationally simple electrochemical deoxygenation method based on the use of an inexpensive zinc cathode in a 2-electrode setup using formic acid as a green solvent and source of protons. This straightforward approach allowed efficient deoxygenation of a variety of aryl-substituted aldehydes and ketones, expanding the scope and efficiency of previously reported methods. Notable highlights in the scope are conversions of biogenic furfural, vanillin and syringaldehyde in good to excellent yields. The simple reaction conditions developed in batch were readily transferred to a more practically relevant flow setup and used for the preparative, multi-gram scale preparation of deoxygenated value-added products. Systematic studies showed good reusability of all components of the reaction setup, like electrodes.

Green foundation

1. We report a mild, safe, sustainable, and operationally very simple electrochemical Clemmensen-type carbonyl deoxygenation method of various aryl aldehydes and ketones, including biomass-derived vanillin and furfural. The reaction proceeds without excess reagents and hazardous reagent waste, like amalgamated zinc, hydrazine, or compressed hydrogen gas.
2. The efficient electrochemical process, employing formic acid as a green solvent, reusable electrodes, and electricity as a renewable reducing agent, showed good yields for the deoxygenation of more than 40 compounds in batch-type cells and excellent yields for the gram-scale deoxygenation reactions of vanillin and syringaldehyde in a flow electrolysis system. With its practicality, this process opens up an opportunity to obtain higher-value chemicals or fuel additives from simple biomass-derived carbonyl compounds.
3. In the future, further developments in metal-free carbon-based electrodes as well as valorizing anodic counter reactions may be investigated. The preparative synthesis can be applied to the deoxygenation of many other types of organic compounds.

Introduction

Biomass-derived carbonyl compounds represent appealing platform chemicals due to their abundance and structural diversity. In particular, aromatic aldehydes from lignocellulosic biomass, such as furfural, vanillin, and syringaldehyde, offer promising opportunities for their valorisation into higher-value chemicals, materials, or fuel additives (Fig. 1, left).[1–5]

To date, many impressive transformations have been developed from these biomass-derived aldehydes giving access to compounds utilized across multiple industries. However, some of their transformations remain challenging. Among them is the deoxygenative reduction of the carbonyl group to the methylene moiety (Fig. 1, middle), which is particularly difficult for sensitive substrates like furanic compounds[6–11] due to their tendency to undergo hydrolysis[12,13] or polymerization.[14,15] Despite these challenges, the resulting 2-methylfuran has market potential as a biofuel additive, and its further reduced products, tetrahydrofuran analogues and diols, are valuable compounds as solvents and precursors in the polymer industry.[16–19] Therefore, the development of a sustainable, efficient, and chemoselective synthetic route for this transformation remains a high-value objective in modern synthetic chemistry.

The classical carbonyl deoxygenation protocols in organic chemistry, namely Wolff–Kishner and Clemmensen

[a]Max-Planck-Institute for Chemical Energy Conversion, Stiftstraße 34–36, 45470 Mülheim an der Ruhr, Germany. E-mail: siegfried.waldvogel@cec.mpg.de; Tel: +49 208/306-3131
[b]BASF SE, 67056 Ludwigshafen, Germany
[c]Karlsruhe Institute of Technology, Institute of Biological and Chemical Systems – Functional Molecular Systems (IBCS-FMS), Kaiserstraße 12, 76131 Karlsruhe, Germany

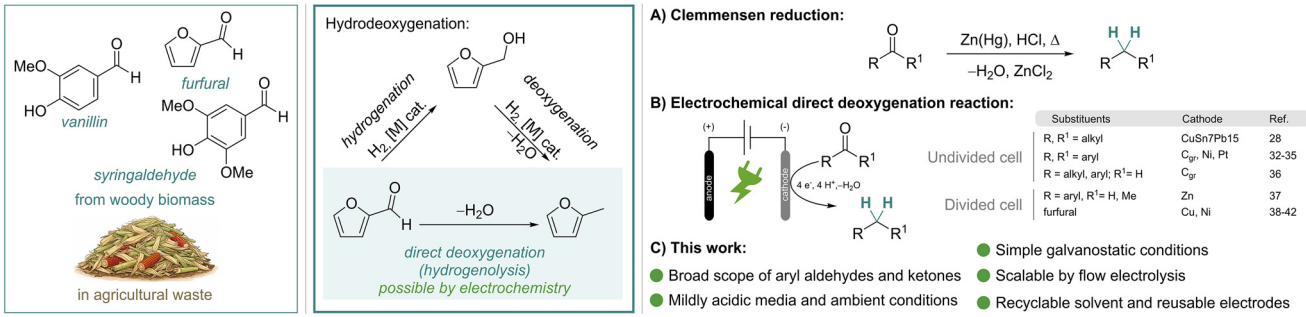

Fig. 1 Aldehydes derived from woody biomass found in agricultural waste (left). Reduction pathways of the aldehyde group of furfural: two-step hydrodeoxygenation and direct deoxygenation (middle). Classical Clemmensen and electrochemical approaches for deoxygenation (right).

reductions,[20,21] rely on the use of a large excess of toxic reagents and generally harsh reaction conditions. For example, the Clemmensen reaction (Fig. 1A) requires highly toxic mercury-containing amalgamated zinc, as well as concentrated and corrosive HCl. Such conditions do not represent only a safety risk and environmental concern but also limit functional group tolerance and thereby the general applicability of the method (*e.g.*, it is not suitable for furfural). A more general alternative approach is based on a two-step hydrodeoxygenation strategy (Fig. 1, middle). Typically, it requires the presence of a homogeneous or heterogeneous transition metal catalyst. They are often based on costly precious metals, along with elevated reaction temperature and high hydrogen pressure. This requires an expensive and safety relevant laboratory setup. Under these conditions, undesirable side reactions such as dehalogenation with halo-substituted substrates or saturation of multiple bonds and aromatic entities are not uncommon.[22]

Among modern approaches, electrosynthesis proved itself as an especially powerful tool enabling the direct deoxygenation under mild conditions (Fig. 1B). In general, electrochemical methods provide unique advantages in terms of inherent process safety, sustainable use of resources, a lower amount of generated metal waste, and the possibility to consume intermittent variable renewable energy and thereby stabilize the electrical grid.[23–25] The lower amount of metal waste generated not only makes the process more cost-efficient but also lowers metal contamination of the products obtained and makes purifications less demanding.

Our group reported an example of benzamides and sulfoxide deoxygenations at a lead cathode already more than a decade ago.[26,27] Recently, we reported a more sustainable example of direct deoxygenation of alkyl substituted ketones in an undivided cell under galvanostatic conditions by utilizing a leaded bronze cathode.[28–31] Other notable electrochemical methods for direct deoxygenation of aryl ketones include reactions in undivided cells at graphite, nickel, or platinum cathodes.[32–35] Despite significant progress, these methods are not compatible with aldehydes. These substrates were only tolerated in an undivided setup when the system relied on the dissolution of a sacrificial anode, thereby generating a significant amount of waste. The reaction also works only in fluorinated alcohol as a solvent which limits its practicality for large-scale applications.[36]

Alternatively, using a divided cell, the direct deoxygenation was performed under potentiostatic conditions using zinc as a cathode material, which was reported by the Choi group.[37] While effective for aryl aldehydes, the method operates at low substrate concentrations in strongly acidic aqueous media and requires $NaClO_4$ as a supporting electrolyte.

Beyond vanillin and syringaldehyde, the deoxygenation of furfural derivatives is of huge interest, yet remains challenging. Few representative reports include the successful work on deoxygenation of furfural, mostly on the Cu electrode. However, these methods are not focused on the synthetic preparative aspect of electrolysis.[38–42]

Despite all the impressive developments in the cathodic deoxygenations, we recognized a need for a general scalable electrochemical method applicable to aldehydes and, within this class especially, biomass-derived aldehydes. To address this challenge, we report a general and synthetically useful Clemmensen-type electrochemical deoxygenation of both aldehyde and ketone functional groups. This transformation is performed on a readily available zinc cathode and employs formic acid as the solvent. Importantly, the reaction proceeds efficiently under ambient conditions, offering a practical and operationally simple approach. To support claims of scalability and practicality, we present a development from milligram scale in screening batch-type cells to multi-gram preparative scale in a flow reactor together with product isolation protocols, kinetic studies, and electrode reusability studies.

Results and discussion

Screening in a divided batch-type cell

With scale-up considerations in mind, the deoxygenation was optimized in a simple 2-electrode setup under galvanostatic conditions.[43] As a test substrate, 4-fluorobenzaldehyde (**1a**) was chosen, conveniently allowing the analysis by ^{19}F NMR of crude reaction mixtures in the initial screening. Moreover, halo substituted substrates are considered challenging as they

Table 1 Electrochemical deoxygenation of **1a** [a]

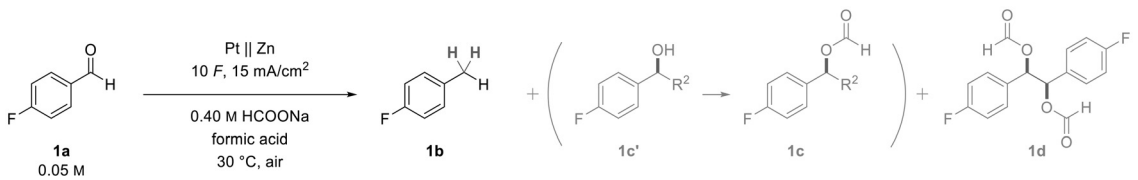

Entry	Deviation from standard conditions	Yield **1b** [%]	Yield **1c** [%]	Yield **1d** [%]
1	None	78	10	0
2	Undivided cell	6	10	16
3	Glass frit as a separator instead of Nafion™ N324	68	7	6
4	Stainless steel, Cu, CuSn7Pb15 as a cathode	1	3–15	0–30
5	Ni foam, BDD as a cathode	0	1–11	0–25
6	No supporting electrolyte in the catholyte	74	11	0
7	NBu_4BF_4, NEt_4BF_4, H_2SO_4, HCOOK instead of HCOONa	66–77	13–24	0
8	BDD, graphite, DSA or GC as an anode	72–77	8–13	0
9	24 h without electricity	1	2	0

[a] Reaction conditions: anolyte 2.8 mmol of HCOONa in 7 mL of formic acid, catholyte 0.35 mmol of 4-fluorobenzaldehyde (**1a**) and 2.8 mmol of HCOONa in 7 mL of formic acid. Reactions were performed using a platinum anode and a zinc cathode, 15 mA cm^{-2}, 10 F in a divided cell (Nafion™ N324) at 30 °C under air. The reported current density is calculated based on the geometric area of the electrode. ^{1}H NMR yields were determined using 1,3,5-trimethoxybenzene as the internal standard. Further details are reported in Table S1. BDD, boron-doped diamond; DSA, dimensionally stable anode (IrO_2 on Ti); GC, glassy carbon.

showed only limited success in the previous electrochemical deoxygenation studies.[44]

To expand the scope of prior methods, we selected formic acid as a solvent for its ability to donate protons, form hydrogen bonds, and thus activate the carbonyl group and stabilize intermediates, while also serving as a conductive medium. Green routes to formic acid are the electrochemical reduction of carbon dioxide or biomass conversion methods.[45,46] A successful cathodic deoxygenation of **1a** under galvanostatic conditions was indeed achieved in a divided batch-type screening cell with Zn as the cathode,[47] an applied charge of 10 *F* at a current density of 15 mA cm^{-2} with sodium formate as a supporting electrolyte (78% yield, Table 1). The test reaction exhibited high selectivity, providing only 10% yield of 4-fluorobenzyl formate (**1c**) aside from the formation of the desired **1b** (Table 1). Accordingly, this corresponds to an 88% selectivity for **1b** over **1c**. Moreover, no pinacol byproduct was detected under these electrochemical conditions (Table 1). All the initial reactions were conducted in a divided-type cell using a sulfonic acid-based cation exchange membrane (Nafion™ N324) as a separator to avoid undesired oxidative transformations of the starting material **1a** lowering the yield of **1b** (entry 2, Table 1). Indeed, the control experiment in an undivided cell furnished a trace amount of the desired **1b** (6% yield) in addition to the byproduct **1c** in 10% yield, pinacol **1d** in 16% yield, and other products, likely resulting from anodic oxidative transformations (Table 1). Alternatively, a glass frit can be used as a separator giving a slightly decreased yield of 68% (entry 3).

Other cathode materials, like stainless steel, copper or leaded bronze (CuSn7Pb15) were found to yield only a trace amount of the product (1%, entry 4, Table 1 and Table S1). Low yields for Cu and CuSn7Pb15 are especially surprising as they have been previously reported in deoxygenated reduction reactions of alkyl and aryl carbonyl groups.[28,37,48,49] No formation of **1b** was observed when nickel foam or boron-doped diamond (BDD) was used as the cathode (entry 5, Table 1). The reaction without the supporting electrolyte HCOONa in the catholyte led to overheating due to poorer conductivity, although the reaction yield remained almost unaffected (74% yield, entry 6, Table 1). Other supporting or strong electrolytes, such as NBu_4BF_4, H_2SO_4, HCOOK, had a slightly detrimental effect on the yield of **1b** (entry 7 in Table 1), with NEt_4BF_4 being the only supporting electrolyte to yield **1b** in 77% (see Table S1). Lowering the amount of NEt_4BF_4 in the catholyte decreased the yield slightly to 72% (see Table S1), demonstrating that alkyl ammonium salts are a suitable alternative to alkali formates for this type of transformation. We continued with sodium formate as the supporting electrolyte of choice due to its low cost and simple subsequent purification process.

The clean decarboxylative counter reaction of sodium formate in the anolyte (Scheme S1) worked well with multiple electrodes.[50,51] Of the anodes tested, glassy carbon (GC) provided a result comparable to Pt, but the electrode was not used further due to colour changes on the surface upon a single electrolysis (entry 8, Table 1). Other electrodes like BDD,[52,53] dimensionally stable anode (DSA, IrO_2 on Ti),[54,55] and graphite gave approximately 5% lower yields. Therefore, we continued using Pt as the anode.

Lastly, the control experiment conducted without electricity and 12-fold longer reaction time revealed only traces of conversion to **1b** (1%, entry 9, Table 1). A control electrochemical reaction starting from 4-fluorobenzyl alcohol (**1c′**) did not yield any **1b** ruling out **1c′** as an intermediate (Scheme S3).

Influence of solvent mixtures

With the optimized reaction conditions described in Table 1, the influence of solvent mixtures was investigated (Fig. 2). The

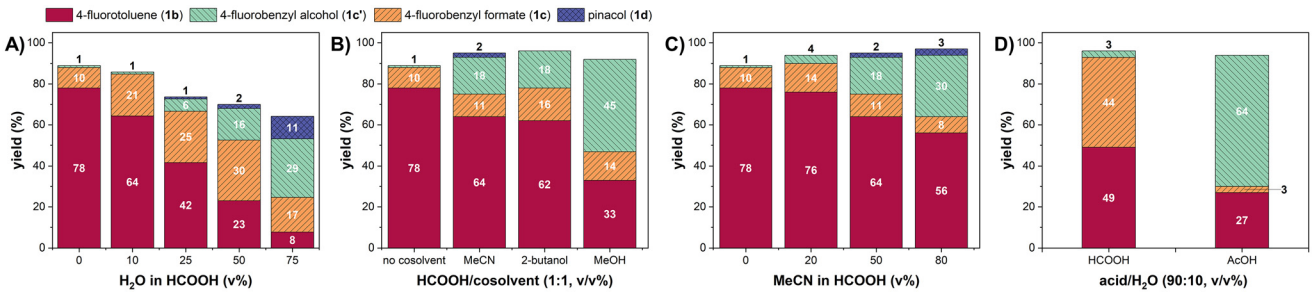

Fig. 2 Influence of solvent mixtures with formic acid on the yield of reductions (A–D): different amounts of H_2O (A), different organic solvents (B), different amounts of MeCN (C), comparison of reactions at 7 mA cm^{-2} in aqueous solutions of formic and acetic acid, with NBu_4BF_4 as a supporting electrolyte (D). In the case where acetic acid was used, 4-fluorobenzyl acetate was formed instead of 4-fluorobenzyl formate.

aim of these experiments was to identify compounds applicable to substrates that are either insoluble in pure formic acid or sensitive to the acidity of the electrolyte system. When formic acid was diluted with water, the yields of **1b** decreased: the larger the amount of water, the lower the yield (Fig. 2A). Apart from giving the lowest yield of deoxygenation, the HCOOH/H_2O mixture (25 : 75, v/v%) also gave the highest yield of the hydrogenation product 4-fluorobenzyl alcohol (**1c′**), which, under these reaction conditions, was not immediately esterified to the corresponding 4-fluorobenzyl formate (**1c**).

The 1 : 1 mixture of formic acid with acetonitrile instead of water showed a higher yield (64%). However, it was still 14% lower than the reaction in formic acid (Fig. 2B). A similar observation was made with 2-butanol[56] (62% yield), but not with MeOH as solvent which resulted in a significantly lower yield of 33%. The significant difference in yields could be attributed to hindered formation of the acetal in the case of sterically bulkier 2-butanol.

Based on these results, we tested the best performing cosolvent acetonitrile in different ratios with formic acid. With progressively higher amounts of acetonitrile, the yields drop from 78% in pure acid to 56% of **1b** in the formic acid–acetonitrile mixture (20 : 80). The formic acid–acetonitrile mixture (80 : 20) turned out to give a high 76% yield, which gives the opportunity to react compounds that are poorly soluble in pure formic acid.

The superiority of formic acid for deoxygenation-type reactions is proven when compared to reactions using acetic acid (Fig. 2D). In strong contrast to formic acid, the acetic acid system required the addition of water or another supporting electrolyte to achieve the desired constant current. To compare the reaction yields in formic and acetic acid, the optimized reaction conditions were slightly adapted to account for low NaOAc solubility and therefore poor conductivity (7 mA cm^{-2} and NBu_4BF_4 instead of 15 mA cm^{-2} and HCOONa). The results show that the medium with a higher pH worked selectively well only for hydrogenation to the alcohol **1c′** (64% yield) but not for hydrogenolysis to **1b** (27% yield).

Notably, no signs of zinc electrode decomposition caused by electrolysis were observed in either pure formic acid or any of the tested solvent mixtures.

Design of experiments

Using a full factorial 2^3 Design of Experiments (DoE),[57] the influence of the electrochemical parameters on the yield of **1b** was systematically investigated.

The ranges for the selected parameters—amount of applied charge, current density, and amount of **1a**—were broadly set at 4–10 *F*, 3–33 mA cm^{-2}, and 0.2–1.8 mmol (0.03–0.26 M), respectively (Tables S2 and S3). The optimal electrolysis parameters for the batch-type reaction, which experimentally gave 79% yield (Table S4), were found to be: 10 *F* of amount of applied charge, 15 mA cm^{-2} of current density, and 0.2 mmol of **1a** (Fig. S4). As seen from the Pareto chart (Fig. S4), the highest statistically significant influence on the reaction yield came from the two cross-interactions: current density–concentration and amount of applied charge–concentration. The concentration alone was also found to have a statistically significant influence.

Based on the results obtained, we decided to use the highest amount of applied charge, 10 *F*, and optimal current density of 15 mA cm^{-2}. Although, according to the DoE, the most diluted solution (0.03 M) gives the highest yield, we continued our investigations with the more practical and slightly increased concentration of the starting material **1a** (0.05 M), with which we still observed comparably high yields of the transformations as described below.

Synthetic application

With the optimized conditions in hand, the general applicability of the method was systematically evaluated on different organic carbonyl compounds (Scheme 1). Firstly, the effect of the position of the fluorine substituent on the aromatic ring was investigated: *p*- and *o*-fluorobenzaldehydes (**1a** and **2a**) gave better reaction yields (78% and 56%), whereas electrolysis of *m*-fluorobenzaldehyde (**3a**) resulted in 30% yield of **3b**. Similar to the test substrate **1a**, other halogenated *p*-Cl and *p*-Br benzaldehydes could also be deoxygenated with around 50% yield (**4b** and **5b**), with notably only 4-iodobenzaldehyde (**6a**) showing loss of the halo substituents but to a low degree. When the compounds with one electron-releasing group were subjected to the reaction conditions, the observed yields were significantly higher. For example, 4-hydroxybenzaldehyde was

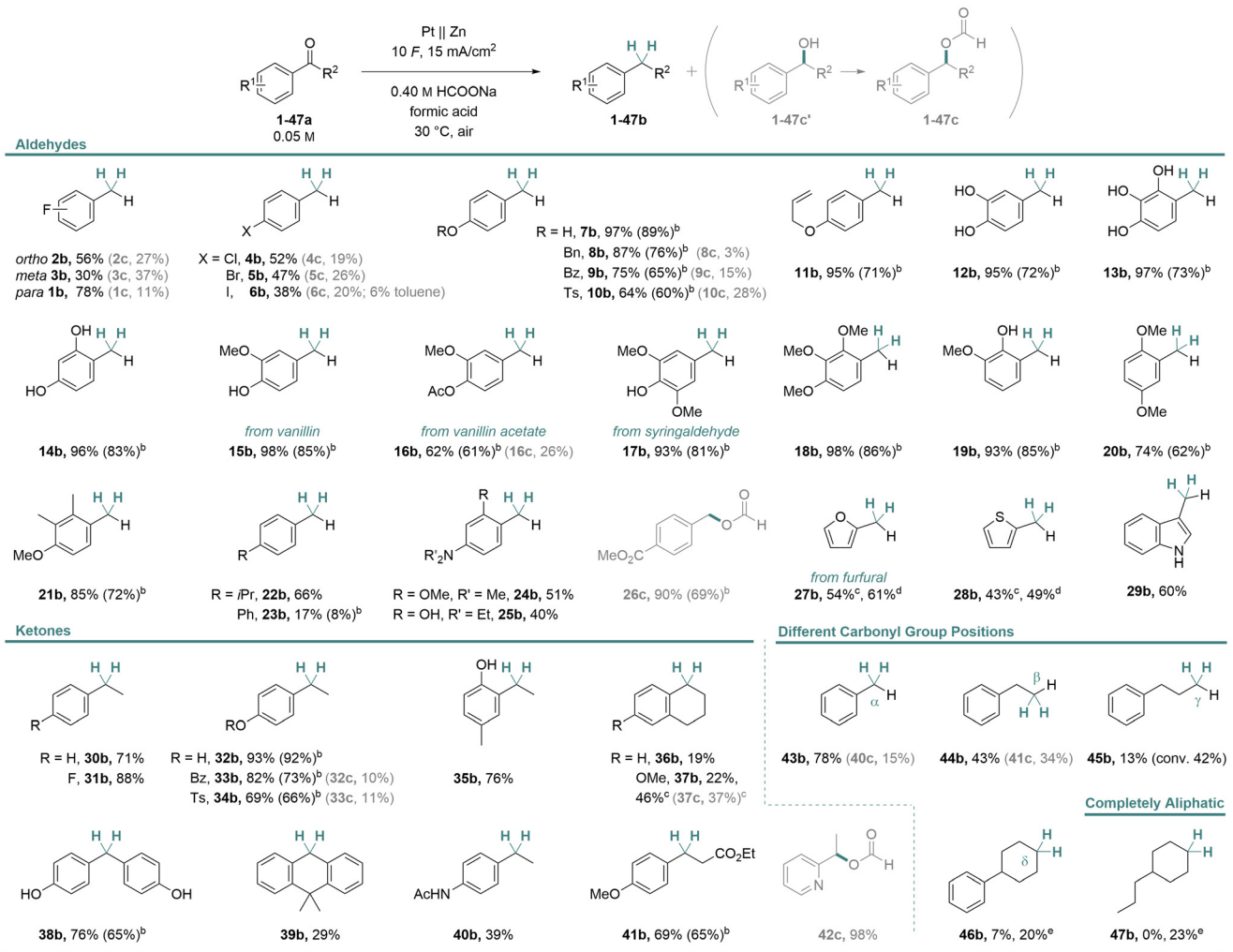

Scheme 1 The synthetic scope of the developed electrochemical deoxygenation. Reaction conditions: anolyte 2.8 mmol of HCOONa in 7 mL of formic acid, catholyte 0.35 mmol of carbonyl substrate and 2.8 mmol of HCOONa in 7 mL of formic acid. Reactions were performed using a platinum anode and a zinc cathode, 15 mA cm^{-2}, 10 *F* in a divided cell (Nafion™ N324) at 30 °C under air. The reported current density is calculated based on the geometric area of the electrode. ^{1}H NMR yields were determined using 1,3,5-trimethoxybenzene as the internal standard. [a] Reported are isolated yields. [b] Formic acid/MeCN (1 : 1). [c] Formic acid/2-butanol (1 : 1). [d] Addition of $AlCl_3$ (1.3 equiv.) in formic acid/MeCN (4 : 1), not isolated.

deoxygenated in almost quantitative 97% yield (**7b**). For the benzyl-protected hydroxyl group, the deoxygenation yield remained high (87% for **8b**). This example shows the complementarity of the developed method and classical hydrogenation conditions, under which the benzylic protecting group is commonly cleaved. Moreover, the benzoyl ester group, which is not stable under Wolff–Kishner reaction conditions, was tolerated as well, with 75% yield of compound **9b**. Tosylated 4-hydroxybenzaldehyde reacted with 64% yield of **10b** and a higher amount of unwanted ester **10c**. The high yield of **11b** (95%) demonstrates the remarkable tolerance of the double bond under the applied reaction conditions. Notably, reactions with the biomass-derived benzaldehydes worked exceptionally well under the developed electrochemical conditions. Because of their electron-rich nature, observed ^{1}H NMR yields were all above 90% (**12b–19b**). This includes vanillin and syringaldehyde, which showed isolated yields of 85% for **15b** and 81% for **17b**, respectively. Benzaldehyde containing the alkyl moiety, namely the isopropyl entity, furnished the product **22b** with a yield of 66%, while the aldehyde containing the biphenyl moiety underwent deoxygenation with a **23b** yield of only 17%. In the case of amine-substituted substrates (**24a** and **25a**), the acidic medium leads to the conversion of the otherwise electron-releasing group, basic tertiary amine, into a protonated and thereby electron-withdrawing group, which makes reduction to alcohol more likely.[44] In these cases, the observed deoxygenation yields were therefore slightly lower (51% and 40% for **24b** and **25b**, respectively). With a strongly electron-withdrawing carbonyl ester substituent, we observed only hydrogenation product **26c** in high 90% yield.

A special emphasis was put on the heterocycles furfural (**27a**) and 2-thiophenecarboxaldehyde (**28a**). These required some additional optimization of reaction solvents due to their instability in neat formic acid (Fig. S6 and S7). The successful

deoxygenations were obtained with the 1 : 1 mixtures of formic acid with either acetonitrile or 2-butanol. This way, 54% or 61% of 2-methylfuran (**27b**) and 43% or 49% of 2-methylthiophene (**28b**) were achieved, respectively. The deoxygenation reaction of furfural (**27a**) also worked in 1 : 1 mixtures of formic acid with green solvents dimethyl carbonate (50%) and 2-MeTHF (63%, Fig. S6). This method also worked with indole-3-carbaldehyde (**29a**), a biologically active metabolite, giving skatole (**29b**) in 60% yield.

Our method is not limited only to aldehydes; the carbonyl group of ketones is also a suitable structural motif for deoxygenation. The deoxygenation of acetophenone **30a** and its fluorinated derivative **31a** proceeded well, giving very good yields (71% and 88%, respectively). Similarly, as observed before with aldehydes, the electron-releasing hydroxyl group on the *para* position was also beneficial for the deoxygenation of acetophenone, which resulted in 93% yield of **32b**. Similarly, protected 4-hydroxyacetophenones underwent deoxygenation in 82% and 69% yields (**33b** and **34b**). Meanwhile, structurally more rigid tetralones **36a** and **37a** gave around 20% yield of deoxygenation to tetralin derivatives **36b** and **37b**, but when the solvent mixture contained 1 : 1 formic acid/acetonitrile, the solubility of **37a** improved and the yield of transformation increased (46% for **37b** and 37% for **37c**). Sterically bulkier hydroxybenzophenone was deoxygenated in 76% yield (**38b**), but anthracenone showed diminished reactivity with only 29% yield of deoxygenation to product **39b**.

Chemoselectivity studies revealed that amidated acetophenone underwent the reaction to afford **40b** in 39% yield, while the ester moiety in **41a** was particularly well tolerated, as the deoxygenation yielded **41b** in 69% yield, with the remaining material recovered as the unreacted starting material.

Similar to the previously observed trend with basic amines, 2-acetylpyridine (**42a**) also underwent protonation of the pyridine ring resulting in the change of selectivity towards hydrogenation product ester **42c**, which was obtained in 98% yield.

Interestingly, the reaction still proceeded when the carbonyl group was shifted from the alpha position to the delta position, relative to the aromatic ring, although the yield decreased with increasing distance (from 78% yield for compound **43b** to 7% for **46b**). The lower reactivity observed for aliphatic aldehydes could result either from more difficult substrate reduction and the predominance of hydrogen evolution or from the lower stability of the reaction intermediates. Reaction with alkyl ketone **47a** worked only with the addition of $AlCl_3$.

For comparison, we selected three representative scope examples and evaluated our reaction system against literature-reported electrolyte systems under galvanostatic conditions.[28,37,44] In this comparison, our system afforded higher deoxygenation yields for all three substrates: 4-fluorobenzaldehyde, vanillin, and furfural (Fig. S8–S11) following the general reactivity pattern, consistent with the reactivity reported by the Choi group. Electron-donating substituents lead to deoxygenation, while electron-withdrawing substituents accelerate alcohol formation due to enhanced stabilization of the corresponding reaction transition state.[44] Importantly, on comparing the selectivity of these two pathways, in all the cases, our system exhibited significantly higher deoxygenation selectivity over hydrogenation than the previously reported solvent system (Fig. S9 and S11). The exact origin of the enhanced deoxygenation selectivity in our system remains unclear at this stage. Our voltammetric studies showed reduction of benzylic carbonyls prior to proton reduction, together with slightly suppressed hydrogen evolution, indicating interaction of the intermediates with the zinc surface (Plot S1). The nature of the subsequent transformation remains uncertain. Notably, none of the investigated scope examples showed insertion or dimerization by-products that would support the carbene-type mechanism under our conditions as previously proposed in the report by Liu.[36]

Overall, the showcased stability of halo substituents, ethers, alkenes, esters, benzyl, sulfonyl, phenol, amide, and amine functional groups as well as heterocycles suggests that the reported method is indeed mild and broadly applicable.

Stability of electrodes and surface analysis

For the use of zinc as a cathode material in a large-scale technical electrolyser, the reaction reproducibility and the electrode stability become very important factors. To get this information, we conducted a systematic study by running eight consecutive reactions in a batch-type setup and monitored the surface changes with scanning electron microscopy (SEM).

During the experimental sequence with rinsing and without polishing of the zinc cathode after each run, zinc proved to be a reliable and stable material for the reported hydrogenolysis of 4-fluorobenzaldehyde (**1a**). Performing eight consecutive reactions with the same, previously unused zinc electrode showed minor fluctuations in yields (76%–82%) of **1b** and unchanged ratios between **1b** and **1c** (Fig. S12).

The yield did not change even when the sequence of eight experiments was repeated with a zinc electrode that was previously used for at least 20 times (Fig. S12). Although the results show that electrode polishing prior to the reaction is not necessary for obtaining the reproducible yields, the SEM images show some changes on the surface of the material after the electrolysis (Fig. 3D). These changes resemble the surface of the electrode after the control experiment without electricity (Fig. 3C). The surface of the electrode is restored to its initial appearance after gentle polishing with sandpaper (Fig. 3F).

Interestingly, upon introducing $ZnCl_2$ as an additive (1 equiv.) during the electrolysis, the product selectivity changed significantly: the hydrogenolysis yield decreased to 44% yield of **1b**, while the hydrogenation yield increased to 34% yield of **1c**, effectively resulting in a drop in overall selectivity from 88% to 56% (Table S5). However, in this experiment, the cathode surface noticeably changed, getting covered with large chunky zinc deposits. This suggests that if Zn^{2+} is present in the solution, it is reduced to Zn^0 under the applied potential during electrolysis and redeposited back onto the electrode. These findings are consistent with the ICP-OES analysis reported on a similar system by the Choi group, which shows only a negligible amount of Zn^{2+} ions in the solution after the

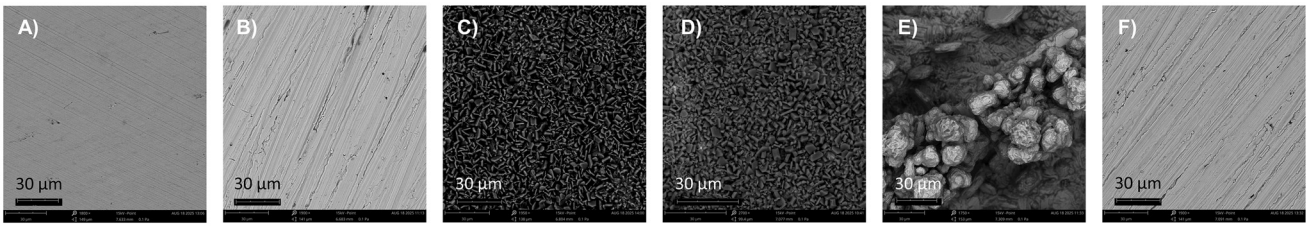

Fig. 3 SEM images of zinc electrodes before and after electrolysis (A–F). Zn electrode as received (A). Zn electrode after first polishing (B). Zn electrode after being in a reaction solution without applied electricity (C). Zn electrode after electrolysis (D). Zn electrode after reaction performed with $ZnCl_2$ as an additive (E). Zn electrode after electrolysis and electrode preparation (F).

electrochemical reaction.[37] Under the electrolysis conditions, the electrode remains largely intact over time as a consequence of the applied potential which prevents the dissolution.

Transfer to flow electrolysis

In order to make the reaction more scalable and practically relevant, the process was transferred from batch-type cells to a continuous flow electrolysis setup. The benefits of flow include more efficient mass transport, heat dissipation, and decreased ohmic resistance of the cell, which results in a lower cell operating voltage.[58–63] Consequently, a flow-based electrolysis system provides a more robust and cost-efficient platform for reproducible scale-up. The method was developed in a divided-cell flow-type system operated in recirculating mode, employing a cathode with a 12 cm^2 surface area (Table S7, see the SI for technical data).

The first experiments in flow were conducted using vanillin (**15a**) as a starting material since it is an inexpensive, biomass-derived compound,[64,65] and its deoxygenated product creosol (**15b**) has its use as a flavouring and fragrance agent.[66,67] Notably, all experiments described below were conducted without the addition of a supporting electrolyte in the catholyte, as the low interelectrode gap enabled sufficiently high conductivity.

Transferring the reaction parameter from batch to flow directly, without any additional optimization resulted in slightly diminished yields of **15b** compared to batch-type electrolysis (83% *vs.* 98%, respectively, see Table S7 and Scheme 1). Next, the focus of additional optimization efforts in flow was on improving the yield and practicality of the system by increasing the concentration and current density. The first has an influence on lower consumption of solvents during electrolysis and easier work-up, and the latter on the yield by electrolysis time and thereby productivity. Relative to the batch-type conditions, the vanillin (**15a**) concentration was scaled by factors 2, 4, and 8 (entries 1–4, Table S7), while the applied current was similarly increased by 2-, 4-, 6-, and 8-fold (entries 4–8, Table S7). Increasing the substrate concentration led to a pronounced improvement in **15b** yield, reaching up to 97% yield (entry 4, Table S7). More importantly, current density could be raised substantially to 60 mA cm^{-2} while maintaining a high yield of 94% (entry 6, Table S7). Further increases of current densities proved to be detrimental for current efficiency, as evidenced by a yield decrease (85% yield of **15b** for 120 mA cm^{-2}, Table S7).

Reaction kinetic study and reproducibility in flow

Encouraged by the excellent performance observed in the flow cell, we conducted a systematic evaluation of reaction kinetics and compared the results with two different current densities: 15 and 60 mA cm^{-2} at the highest investigated concentration of 0.40 M (Fig. 4A and S13). The monitoring of product buildup over time was performed to provide insights into the reaction rate, as well as the current efficiency.

The kinetic plot reveals that the same amount of **15b** (48%) is synthesized in the first 2 *F*, no matter if 15 or 60 mA cm^{-2} is used. With the increasing amount of the applied charge, the differences in the yield of **15b** became more significant depending on the selected current density. At 15 mA cm^{-2}, conditions turned out to be optimal for obtaining the highest yield and at 60 mA cm^{-2}, optimal for high productivity (Fig. 4A, B and S14, 15).

The obtained kinetic plot at 15 mA cm^{-2}, shown in Fig. 4B, also indicates that the maximum current efficiency is achieved at 2 *F* (96%), which gradually decreases with a large amount of applied charge. Upon passage of 4 *F*, the theoretical requirement for the deoxygenation reaction, the yield of **15b** reaches 89%. However, 4 *F* is insufficient for complete conversion, as also observed in the DoE study, where a significant amount of starting material **1a** remained unreacted in the batch-type cell (Table S3). To achieve full conversion for the envisioned large-scale synthesis, the amount of applied charge was increased, with the maximum yield (99% for **15b**) obtained after applying 7 *F* (Fig. 4B). Further increase of the amount of applied charge beyond 7 *F* did not improve the yield and only led to hydrogen formation. Similar to batch conditions, we continued to study the electrode reusability and reaction reproducibility. Consecutive reactions were carried out in a flow cell, with the cell being rinsed between each run, and the flow set-up disassembled for inspection between the fifth and sixth runs. Over the course of six consecutive reactions, the hydrogenolysis yield remained consistently high (97–99%, Fig. 4C), highlighting both the outstanding durability of the electrode and the reproducibility of the process. In the case of a reproducibility study at a higher current density of 60 mA cm^{-2}, 10 *F* of applied charge was needed for the average yield of 94% for

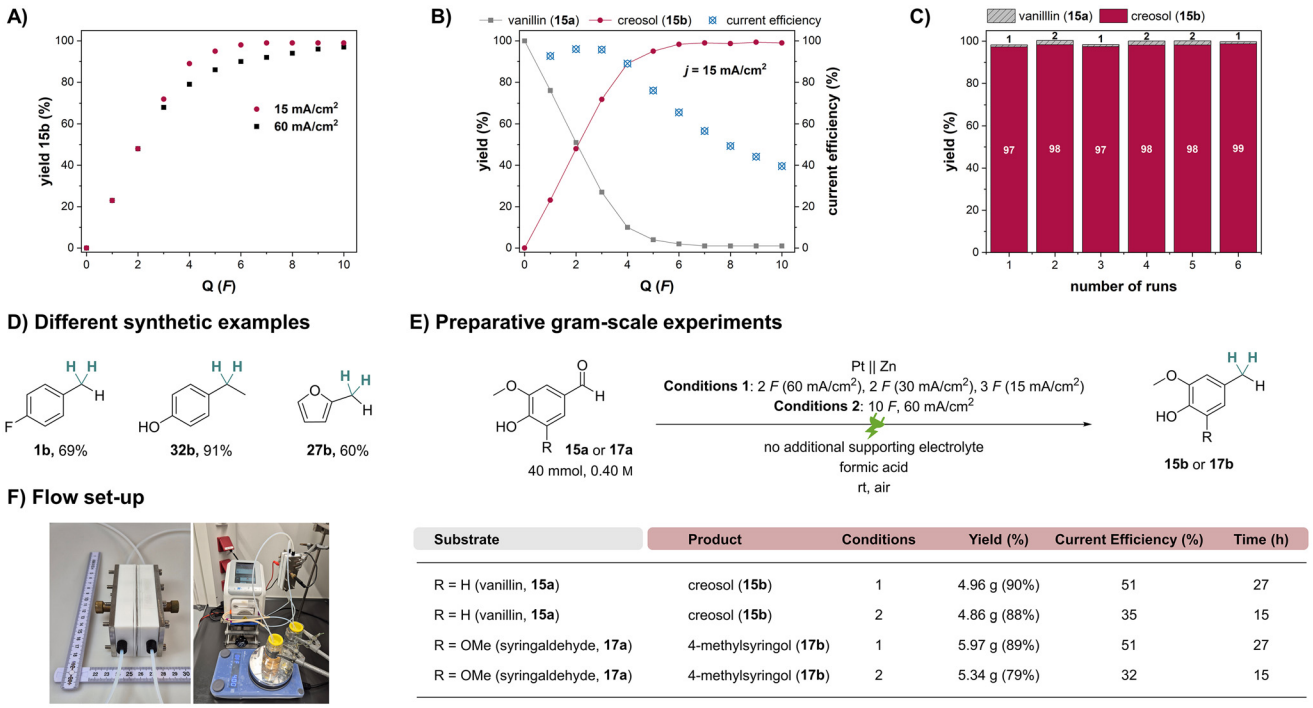

Substrate	Product	Conditions	Yield (%)	Current Efficiency (%)	Time (h)
R = H (vanillin, **15a**)	creosol (**15b**)	1	4.96 g (90%)	51	27
R = H (vanillin, **15a**)	creosol (**15b**)	2	4.86 g (88%)	35	15
R = OMe (syringaldehyde, **17a**)	4-methylsyringol (**17b**)	1	5.97 g (89%)	51	27
R = OMe (syringaldehyde, **17a**)	4-methylsyringol (**17b**)	2	5.34 g (79%)	32	15

Fig. 4 Yield of **15b** as a function of the amount of applied charge at different current densities (A). Kinetic study (B) and reaction reproducibility at 15 mA cm^{-2} (C) in flow. Different synthetic examples (D). Preparative gram-scale experiments (E). An assembled divided flow-type cell and a flow-type system operated in recirculating mode. Scale given in cm (F).

15b, however, resulting in lower current efficiency as with 15 mA cm^{-2} (56% *vs.* 38%, Table S8). The reaction was also well reproducible using a higher current density (Fig. S15).

The conditions in flow are quite general and can be applied with small modifications to different examples, leading to yields in the comparable range as in a batch-type cell (Fig. 4D and Tables S10–S12).

Multigram-scale flow electrolysis

Following the optimization, we tested the stability and durability of the system in a multi-hour preparative scale experiment. We increased the amount of starting material from 2.8 to 40 mmol and used the optimized electrochemical conditions without any additional supporting electrolyte in the catholyte.

To circumvent the long reaction time but keep the good current efficiency, we decided to apply dynamic current density (conditions 1: (1) 2 *F*, 60 mA cm^{-2}, (2) 2 *F*, 30 mA cm^{-2}, and (3) 3 *F*, 15 mA cm^{-2}).

Simultaneously, conditions 2 (10 *F*, 60 mA cm^{-2}, Fig. 4E) were tested to compare current efficiencies and productivities for deoxygenation of both **15a** and **17a**.

The electrolysis proceeded smoothly, with no technical issues or fluctuations in cell voltage observed during the 15- and 27-hour experiments (Fig. S16 and S17). All the components of the system (*e.g.* tubing, membrane, cell, electrodes; Fig. 4F) endured the electrolysis without any noticeable visual signs of wear. The products **15b** and **17b**, both known flavouring substances,[67] were obtained in comparable conversions to smaller scale experiments. After the reaction, the easy purification followed: first, the majority of formic acid was removed *in vacuo* and could be recycled after the reaction, the remaining aldehyde (main impurity, about 5%) was removed by the aqueous metabisulfite wash,[68] and no column chromatography was needed to obtain 90% and 88% of isolated pure product **15b** under conditions 1 and 2, respectively (Fig. 4E), successfully demonstrating the scalability of the electrolysis and downstream processing.

In a similar way, **17a** was deoxygenated using conditions 1 and 2 (Fig. 4E, and Tables S9, 14). The electrolysis and consecutive isolation easily furnished 89% and 79% of pure **17b**, respectively.

Overall, the efficiencies were superior under conditions 1, while conditions 2 resulted in peak productivity. Compared to the reaction conditions in the literature, both conditions 1 and 2 show higher current efficiency and practicality (Table S15).

Finally, a large preparative gram-scale electrolysis protocol was compared to a classical Clemmensen reduction of **15a** and evaluated for sustainability (for a detailed evaluation, see SI Chapter 13). The reported electrochemical process aligns well with the principles of green chemistry, not only because of the reusability of the electrodes and recyclable green solvent but also because of lower environmental pollution and higher safety compared to the classical reduction (Fig. 5).

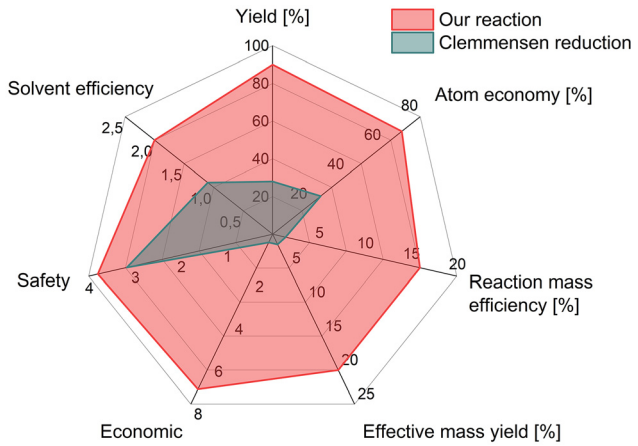

Fig. 5 Radar chart comparing the green chemistry aspects of our method with the classical Clemmensen protocol.

Conclusions

In summary, we have established a novel, mild, efficient, and operationally simple protocol for electrochemical Clemmensen-type carbonyl hydrogenolysis under galvanostatic conditions. The electrolysis is based on the use of a commercially available and inexpensive Zn cathode that can be reused many times without any significant drop of catalytic activity despite some surface changes. In contrast to other electrochemical methods, our protocol does not rely on aqueous media but uses formic acid as a green solvent and proton source. Importantly, this strategy allowed the substrate scope of previous methods to be expanded to various benzaldehyde derivatives, also including those bearing electron-withdrawing substituents (altogether 45 examples). Notable highlights in the scope of the method are multiple abundant biomass-derived aldehydes, including vanillin and furfural. In general, our method shows better yield, selectivity, and current efficiency than previously reported methods. Moreover, the method was readily transferred from a batch to a flow-type setup. Importantly, this setup allowed us to perform electrolysis without any additives in the catholyte compartment due to lower cell resistance. Multi-hour stable operation and potential for further scale-up were demonstrated by successful multigram-scale electrolysis for the preparation of two flavouring chemicals, creosol and 4-methylsyringol. These findings provide a solid framework for future practical application of more sustainable deoxygenation strategies.

Conflicts of interest

There are no conflicts to declare.

Data availability

The data supporting this article have been included as part of the supplementary information (SI). Supplementary information: general procedures and analytical data. See DOI: https://doi.org/10.1039/d6gc02190e.

Acknowledgements

The authors acknowledge the financial support from the BMFTR in the frame of the Cluster4Future ETOS by the project KADIOL (FKZ 03ZU1205CC). The authors gratefully acknowledge technical support from the mechanical workshops at MPI CEC. Support from the Deutsche Forschungsgemeinschaft (DFG, German Research Foundation) – 510228793 – SFB 1633 Project A06 is highly appreciated. The authors also thank Dr Avra Tzaguy for his experimental support in voltammetric studies. The authors acknowledge the use of DeepL Write and ChatGPT (GPT-5, OpenAI) for grammar checking and improving the clarity of the manuscript text, and Adobe Firefly (Firefly Image Model 4) for the generation of the AI-based image of agricultural waste. All scientific content and interpretations were performed by the authors. Open Access funding was provided by the Max Planck Society.

References

1 G. Xu, X. Chen, W. Xu, Q. Shi, Y. Lu and W. Liu, *Green Chem.*, 2026, **28**, 5520–5557.
2 O. He, B. A. Smith, P. Champange, P. G. Jessop and H. Yu, *Green Chem.*, 2025, **27**, 14436–14477.
3 G. Qiang, M. F. Ansari, Z. Sun and S. Elangovan, *Adv. Synth. Catal.*, 2024, **366**, 4805–4834.
4 F. W. S. Lucas, R. G. Grim, S. A. Tacey, C. A. Downes, J. Hasse, A. M. Roman, C. A. Farberow, J. A. Schaidle and A. Holewinski, *ACS Energy Lett.*, 2021, **6**, 1205–1270.
5 G. W. Huber, S. Iborra and A. Corma, *Chem. Rev.*, 2006, **106**, 4044–4098.
6 H. Wen, W. Zhang, Z. Fan and Z. Chen, *ACS Catal.*, 2023, **13**, 15263–15289.
7 R. Mariscal, P. Maireles-Torres, M. Ojeda, I. Sádaba and M. López Granados, *Energy Environ. Sci.*, 2016, **9**, 1144–1189.
8 C. Xu, E. Paone, D. Rodríguez-Padrón, R. Luque and F. Mauriello, *Chem. Soc. Rev.*, 2020, **49**, 4273–4306.
9 Y. Gao, L. Ge, H. Xu, K. Davey, Y. Zheng and S.-Z. Qiao, *ACS Catal.*, 2023, **13**, 11204–11231.
10 J. Carneiro and E. Nikolla, *Annu. Rev. Chem. Biomol. Eng.*, 2019, **10**, 85–104.
11 C. H. Lam, W. Deng, L. Lang, X. Jin, X. Hu and Y. Wang, *Energy Fuels*, 2020, **34**, 7915–7928.
12 J. Horvat, B. Klaić, B. Metelko and V. Šunjić, *Tetrahedron Lett.*, 1985, **26**, 2111–2114.
13 J. J. Roylance and K.-S. Choi, *Green Chem.*, 2016, **18**, 2956–2960.
14 E. de Jong, M. Mascal, S. Constant, T. Claessen, P. Tosi and A. Mija, *Green Chem.*, 2025, **27**, 3136–3166.

15 A. S. Chauhan, O. Singh and P. Das, *Sustainable Energy Fuels*, 2025, **9**, 4775–4792.
16 G. Hayes, M. Laurel, D. MacKinnon, T. Zhao, H. A. Houck and C. R. Becer, *Chem. Rev.*, 2023, **123**, 2609–2734.
17 R. Bijoy, P. Agarwala, L. Roy and B. N. Thorat, *Org. Process Res. Dev.*, 2022, **26**, 480–492.
18 A. T. Hoang and V. V. Pham, *Renewable Sustainable Energy Rev.*, 2021, **148**, 111265.
19 J.-j. Tan, Y.-h. Su, K. Gao, J.-l. Cui, Y.-z. Wang and Y.-x. Zhao, *J. Fuel Chem. Technol.*, 2021, **49**, 780–790.
20 L. Wolff, *Liebigs Ann. Chem.*, 1912, **394**, 86–108.
21 E. Clemmensen, *Ber. Dtsch. Chem. Ges.*, 1913, **46**, 1837–1843.
22 V. S. Prabhudesai, L. Gurrala and R. Vinu, *Energy Fuels*, 2022, **36**, 1155–1188.
23 D. Pollok and S. R. Waldvogel, *Chem. Sci.*, 2020, **11**, 12386–12400.
24 A. Wiebe, T. Gieshoff, S. Möhle, E. Rodrigo, M. Zirbes and S. R. Waldvogel, *Angew. Chem., Int. Ed.*, 2018, **57**, 5594–5619.
25 S. Möhle, M. Zirbes, E. Rodrigo, T. Gieshoff, A. Wiebe and S. R. Waldvogel, *Angew. Chem., Int. Ed.*, 2018, **57**, 6018–6041.
26 C. Edinger and S. R. Waldvogel, *Eur. J. Org. Chem.*, 2014, 5144–5148.
27 J. Kulisch, M. Nieger, F. Stecker, A. Fischer and S. R. Waldvogel, *Angew. Chem., Int. Ed.*, 2011, **50**, 5564–5567.
28 S. Kissel, M. N. Perner, R. Narobe, K. Hochadel, M. Klein, B. Cezanne, P. Schnieders, V. Derdau and S. R. Waldvogel, *Green Chem.*, 2025, **27**, 10801–10807.
29 C. Gütz, V. Grimaudo, M. Holtkamp, M. Hartmer, J. Werra, L. Frensemeier, A. Kehl, U. Karst, P. Broekmann and S. R. Waldvogel, *ChemElectroChem*, 2018, **5**, 247–252.
30 V. Grimaudo, P. Moreno-García, A. Riedo, S. Meyer, M. Tulej, M. B. Neuland, M. Mohos, C. Gütz, S. R. Waldvogel, P. Wurz and P. Broekmann, *Anal. Chem.*, 2017, **89**, 1632–1641.
31 C. Gütz, M. Selt, M. Bänziger, C. Bucher, C. Römelt, N. Hecken, F. Gallou, T. R. Galvão and S. R. Waldvogel, *Chem. – Eur. J.*, 2015, **21**, 13878–13882.
32 C. Bi, X. Zhao, Z. Jia, Y. Chang, H. Yang, M. Song, X. Zhang, Y. Zhang and G. Qing, *ChemCatChem*, 2023, **15**, e202300258.
33 K. Sun, Z. Xu, V. Ramadoss, L. Tian and Y. Wang, *Chem. Commun.*, 2022, **58**, 11155–11158.
34 Y. Wang, J. Zhao, T. Qiao, J. Zhang and G. Chen, *Chin. J. Chem.*, 2021, **39**, 3297–3302.
35 J. Li, L. He, X. Liu, X. Cheng and G. Li, *Angew. Chem., Int. Ed.*, 2019, **58**, 1759–1763.
36 Z. Sun, R. Ji, J. Wu, J. Zhao, F. Fang, F. Wang, C. Jiang and Z.-Q. Liu, *Adv. Synth. Catal.*, 2023, **365**, 476–481.
37 X. Yuan, K. Lee, J. B. Eisenberg, J. R. Schmidt and K.-S. Choi, *Nat. Catal.*, 2024, **7**, 43–54.
38 A. S. Chauhan, O. Singh, Amika, R. Sharma, D. Kumar, D. Kumar and A. Dhanola, *React. Chem. Eng.*, 2025, **10**, 2201–2224.
39 M. Jiang, J. Tan, Y. Chen, W. Zhang, P. Chen, Y. Tang and Q. Gao, *Chem. Commun.*, 2023, **59**, 3103–3106.
40 M. T. Bender, X. Yuan, M. K. Goetz and K.-S. Choi, *ACS Catal.*, 2022, **12**, 12349–12368.
41 A. S. May and E. J. Biddinger, *ACS Catal.*, 2020, **10**, 3212–3221.
42 Y. Kwon, K. J. P. Schouten, J. C. van der Waal, E. de Jong and M. T. M. Koper, *ACS Catal.*, 2016, **6**, 6704–6717.
43 J. Seidler, J. Strugatchi, T. Gärtner and S. R. Waldvogel, *MRS Energy Sustainability*, 2021, **7**, 42.
44 J. B. Eisenberg, K. Lee, X. Yuan, J. R. Schmidt and K.-S. Choi, *J. Am. Chem. Soc.*, 2024, **146**, 15309–15319.
45 N. Yang, S. R. Waldvogel and X. Jiang, *ACS Appl. Mater. Interfaces*, 2016, **8**, 28357–28371.
46 F. Shen, R. L. Smith Jr, J. Li, H. Guo, X. Zhang and X. Qi, *Green Chem.*, 2021, **23**, 1536–1561.
47 C. Gütz, B. Klöckner and S. R. Waldvogel, *Org. Process Res. Dev.*, 2016, **20**, 26–32.
48 X. Yuan, K. Lee, J. R. Schmidt and K.-S. Choi, *J. Am. Chem. Soc.*, 2023, **145**, 20473–20484.
49 A. S. May, S. M. Watt and E. J. Biddinger, *React. Chem. Eng.*, 2021, **6**, 2075–2086.
50 M. Klein and S. R. Waldvogel, *Angew. Chem., Int. Ed.*, 2022, **61**, e202204140.
51 S. B. Beil, D. Pollok and S. R. Waldvogel, *Angew. Chem., Int. Ed.*, 2021, **60**, 14750–14759.
52 S. Lips and S. R. Waldvogel, *ChemElectroChem*, 2019, **6**, 1649–1660.
53 S. R. Waldvogel, S. Mentizi and A. Kirste, in *Radicals in Synthesis III*, ed. M. Heinrich and A. Gansäuer, Springer Berlin Heidelberg, Berlin, Heidelberg, 2012, pp. 1–31, DOI: 10.1007/128_2011_125.
54 F. Sprang, J. D. Herszman and S. R. Waldvogel, *Green Chem.*, 2022, **24**, 5116–5124.
55 Q. Ma and S. Mu, *Interdiscip. Mater.*, 2023, **2**, 53–90.
56 Y. Deng, R. Gao, L. Lin, T. Liu, X.-D. Wen, S. Wang and D. Ma, *J. Am. Chem. Soc.*, 2018, **140**, 14481–14489.
57 M. Dörr, M. M. Hielscher, J. Proppe and S. R. Waldvogel, *ChemElectroChem*, 2021, **8**, 2621–2629.
58 V. Hessel, D. Kralisch, N. Kockmann, T. Noël and Q. Wang, *ChemSusChem*, 2013, **6**, 746–789.
59 T. Noël, Y. Cao and G. Laudadio, *Acc. Chem. Res.*, 2019, **52**, 2858–2869.
60 M. C. Leech, A. D. Garcia, A. Petti, A. P. Dobbs and K. Lam, *React. Chem. Eng.*, 2020, **5**, 977–990.
61 N. Tanbouza, T. Ollevier and K. Lam, *iScience*, 2020, **23**(11), 101720.
62 D. Cantillo, *Curr. Opin. Electrochem.*, 2024, **44**, 101459.
63 R. Narobe, M. N. Perner, M. d. J. Gálvez-Vázquez, C. Kuhwald, M. Klein, P. Broekmann, S. Rösler, B. Cezanne and S. R. Waldvogel, *Green Chem.*, 2024, **26**, 10567–10574.
64 M. Zirbes, T. Graßl, R. Neuber and S. R. Waldvogel, *Angew. Chem., Int. Ed.*, 2023, **62**, e202219217.
65 T. Rücker, T. Pettersen, H. Graute, B. Wittgens, T. Graßl and S. R. Waldvogel, *ACS Sustainable Chem. Eng.*, 2024, **12**, 11283–11296.

66 A. M. Api, D. Belsito, D. Botelho, M. Bruze, G. A. Burton, J. Buschmann, M. A. Cancellieri, M. L. Dagli, M. Date, W. Dekant, C. Deodhar, A. D. Fryer, L. Jones, K. Joshi, M. Kumar, A. Lapczynski, M. Lavelle, I. Lee, D. C. Liebler, H. Moustakas, M. Na, T. M. Penning, G. Ritacco, J. Romine, N. Sadekar, T. W. Schultz, D. Selechnik, F. Siddiqi, I. G. Sipes, G. Sullivan, Y. Thakkar and Y. Tokura, *Food Chem. Toxicol.*, 2021, **153**, 112363.
67 I. C. Munro and B. Danielewska-Nikiel, *Food Chem. Toxicol.*, 2006, **44**, 758–809.
68 M. M. Boucher, M. H. Furigay, P. K. Quach and C. S. Brindle, *Org. Process Res. Dev.*, 2017, **21**, 1394–1403.